明らかに症状が現れたもの、医師が重要と判断したもの等）は有害事象として報告する。
有害事象を認めたときは、直ちに適切な処置、治療を行うとともに、カルテに記録し、症例報告書により報告を行う。

以下のいずれかの要件を満たす入院、又は入院期間の延長は重篤な有害事象とはみなさない。

・２４時間未満の病院滞在（入院とはみなさない）
・事前に予定されていた入院（試験開始前に予定されていた手術によるものなど）
・有害事象とは関連のない入院（例：一時療養目的入院 など）　等

ただし、入院中に行われる侵襲的治療は、医学的に重大とみなされることがあり重篤な有害事象として報告すべきかを臨床的根拠に基づいて判断する。

【重症度の判定】・・・CTCAE 等の判定基準を用いる場合はその旨を記載
個々の有害事象について、次の基準により重症度を判定する。だし、当該事象の臨床的な重要性を考慮する。

・軽度　：日常活動に支障を生じない
・中等度：日常活動に支障はあるが可能
・高度　：日常活動が困難である

【重篤度判定】
個々の有害事象について「２．重篤な有害事象の定義」に従い、重篤度を判定する。

・重篤
・非重篤

有害事象に関するその他調査事項をカルテに記載する

・発生日または発生を認めた日
・消失日または消失を認めた日
・処置の有無と内容
・転帰（消失、残存）
・因果関係（関係あり、なし）
・必要に応じて、併用治療の内容

6.2 有害事象の報告

・有害事象を認めたときは、直ちに適切な処置、治療を行うとともに、カルテに記録し、症例報告書により報告を行う。
・重篤な有害事象を認めたときは、適切な処置、治療を行うとともに、**直ちに**「重篤な有害事象に関する報告書」に所定事項を記入し、病院長に報告する。

6.2.1 重篤な有害事象の報告手順

研究者は直ちに施設の手順に則り、所属長、事務長および病院長へ報告する。

7 研究実施期間

実施承認後～2015 年 8 月 31 日（症例登録期間は 2014 年 8 月 31 日まで）

8 症例数及び設定根拠

目標症例数

網膜色素変性　3 例

症例数の根拠

今回の試験の目的は機器の安全性を調べること、および有効性評価の指標を検討することであり、また機器が高価なため 3 例に設定した。統計的な処理は、電源スイッチの ON 時と OFF 時の成績の差の検定で行うことが可能である。

9 評価項目

9.1 主要評価項目（Primary endpoint）

有効性評価項目：視標の位置の認識の誤差、視標の動きの方向の認識の誤差、縞視力の変化、道標の認識の正解率（デバイスのスイッチＯＮ時、ＯＦＦ時の変化量をアイマスクあり時およびなし時の２条件で測定）

安全性評価項目：前眼部および眼底検査、装置の作動検査、

9.2 副次的評価項目（Secondary endpoint）

有効性評価項目：行動試験（コップと皿の違いの認識、点字ブロックの認識、横断歩道の認識）の正解率（デバイスのスイッチＯＮ時、ＯＦＦ時の変化量をアイマスクあり時およびなし時の２条件で測定）。アンケート調査における点数。脳機能評価（PET 検査、NIRS 検査）

安全性評価項目：蛍光眼底検査（ＦＡ）、眼球運動検査、頭部の術創における有害事象の発生数、光干渉断層計（ＯＣＴ）での網膜厚、経角膜電気刺激（ＴＥＳ）検査での phosphene 閾値

10　統計学的事項

10.1 解析対象集団

10.1.1 有効性解析対象集団

対象として適格と判定し登録され、手術を行った３名を最大解析対象集団と定める。

10.1.2 安全性解析対象集団

登録後、３名の患者のうちその後何らかの安全性データが収集された被験者を安全性解析集団と定める。

10.2 症例・データの取扱い基準

10.2.1 安全性

有害事象については、治療開始から最終治療終了後４週間までに生じたものを解析する。治療開始２週間前～前日までのデータを治療開始前値として取り扱う。ただし複数回検査されている場合は、最も開始日に近いデータを開始前値として扱う。

10.2.2 欠測値

各観察時期の値の欠測値は補完しない。

10.2.3 試験計画違反の取扱い

試験計画違反例で、割り振った条件で治療を行っていない場合は直ちに除外する。
治療は計画どおりであるが検査が計画通りなされていない場合は除外しない。

10.3 解析方法

10.3.1 背景因子

被験者の背景因子に関して、発症年齢、視力が試験時点の視力になった時期を因子として解析する。

10.3.2 有効性評価

10.3.2.1 主要評価解析

臨床所見スコアおよび臨床検査値の変化量または変化率について、装置の電源をONにした時の検査結果とOFFにした時の検査結果をアイマスクあり、なしの各々の条件について統計学的に比較する。

10.3.2.2 副次的解析

行動試験については装置をONにした時とOFFにした時の変化をアイマスクあり、なしの各々の条件について統計学的に比較する。

10.3.3 安全性評価

OCT検査値(網膜厚)については　治療前後の平均値の差の検定を行う。
すべての有害事象を表示し、重篤な有害事象は別途集計する。
なお、因果関係にかかわらず、すべての有害事象についての解析も行う。

11 記録の収集および管理

本研究で用いる記録用紙と提出期限は以下のとおりである。

1) 症例登録票
2) 症例確認書
3) 症例報告書　(観察期間終了後 6 週間以内)

モニタリング

試験が安全に、かつ実施計画書に従って実施されているか、データが正確に収集されているかを確認する目的で、定期モニタリングが行われる。本試験におけるモニタリングは登録責任者が集積される症例報告書の記入データに基づき行う。

モニタリングの項目

1) 集積達成状況
2) 適格性
3) 試験治療/終了状況
4) 重篤な有害事象
5) 有害事象
6) 実施計画書逸脱
7) その他、試験の進捗や安全性に関する問題点

12 倫理的事項

本研究に関与するすべての者は、「ヘルシンキ宣言」および「臨床研究に関する倫理指針」に従って、本研究を実施する。

・ヘルシンキ宣言（2008 年修正版）
・臨床研究に関する倫理指針（平成 20 年改正）
・疫学研究に関する倫理指針（平成 19 年改正）

12.1 インフォームド・コンセント

本研究実施に先立ち、担当医師は倫理審査委員会の承認が得られた説明文書を対象患者に渡し、下記事項を説明したうえで、本研究の参加について自由意思による同意を文書で得る。なお、本研究での研究対象者は重度の視覚障害を有しており、本人が直接署名を行うことが困難であることから、代わりに立会人が署名を行う。

① 研究への参加は任意であること
② 研究への参加に同意しなくても不利益な対応を受けないこと
③ 研究への参加に同意した後でも、不利益を受けることなく撤回することができること
対象患者として選定された理由

④ 研究の意義、目的、方法及び期間
⑤ 多の治療方法の有無
⑥ 研究者等の氏名及び職名
⑦ 研究への参加により期待される利益、起こり得る危険、不快な状態、研究終了後の対応
⑧ 研究に関する資料の入手または閲覧
⑨ 個人情報の取り扱い、研究結果を他の医療機関へ提供する可能性
⑩ 知的財産権の帰属
⑪ 共同研究の場合のその内容
⑫ 費用負担に関すること
⑬ 研究成果の公表
⑭ 研究の資金源
⑮ 関連組織との関わり
⑯ 研究に関する問い合わせ、連絡先
⑰ 補償の有無

12.2 個人情報の保護

研究に関するデータを取り扱う際は、患者の個人情報保護に最大限の努力を払う。
症例報告書を作成する際には、個人を識別する情報の全部または一部を取り除き、代わりに識別コードを付し、連結可能匿名化を行なう。対応表は、個人情報管理者森本　壮が、施錠された書庫にて厳重に保管する。
本研究で得られたデータを当該医療機関外へ提供する際には、対応表は提供せず、連結不可能匿名化されたデータのみを提供する。
学会や論文等で研究成果を発表する場合も、個人を特定できる情報を明らかにすることは決して行なわない。

13 研究費用

13.1 資金源および利益の衝突

本研究は厚生労働省科研費の資金提供を受けて実施するものである。本研究に関して、起こり得る利害の衝突や開示すべき利益相反はない。

13.2 研究に関する費用

本研究期間中の治療にかかる医療費は、観察・検査も含めて厚生労働省科研費でカバーされる。

14 健康被害に対する補償

本研究の実施に伴い、健康被害が生じた場合、研究担当医師は速やかに適切な治療、その他必要な措置を講じ、提供される治療には健康保険を適用する。
機器の不具合以外の原因でこの研究に起因した健康被害が生じた場合、当研究グループが加入す

る臨床研究保険で補償される。また、機器の不具合に起因した健康被害が生じた場合は、(株)ニデックが加入する臨床試験のＰＬ保険で補償される。

15 試料等の利用と保存

該当なし

16 研究成果の公表

本研究の結果は、しかるべき学会に発表し、論文として報告する。学会発表および論文投稿に関しては、研究責任者及び担当者により協議し、決定する。

17 研究組織

責任研究者

不二門尚　大阪大学医学部　感覚機能形成学（眼科兼担　）教授　　06-6879-3941

分担研究者

西田幸二　大阪大学医学部　眼科学　教授　　06-6879-3451

吉峰俊樹　大阪大学医学部　脳神経外科学　教授　　06-6879-3650

瓶井資弘 大阪大学医学部　眼科学　准教授　　06-6879-3452

貴島晴彦　大阪大学医学部　脳神経外科学　講師　　06-6879-3652

坂口裕和　大阪大学医学部　眼科学　助教　　06-6879-3456

森本　壮　大阪大学　　医学系研究科　感覚機能形成学　准教授　　06-6879-3941

圓尾知之　大阪大学医学部　脳神経外科学　助教　　06-6879-3652

神田　寛行　大阪大学　　医学系研究科　感覚機能形成学　助教　　06-6879-3941

18 参考文献

1. Humayun MS, Dorn JD, da Cruz L, Dagnelie G, Sahel JA, Stanga PE, Cideciyan AV, Duncan JL, Eliott D, Filley E, Ho AC, Santos A, Safran AB, Arditi A, Del Priore LV, Greenberg RJ; ArgusII Study Group. Interim results from the international trial of Second Sight's visual prosthesis.Ophthalmology. 2012;119:779-88
2. Zrenner et al., Subretinal electronic chips allow blind patients to read letters and combine them towords. Proc R Soc B 2010; 1-9.
3. Santos,Humayun, M., deJuan, E. Greenburg, R., Marsh, M. Klock, I., Milam, A. Preservation of the Inner Retina in Retinitis Pigmentosa. Arch Ophthalmol 1997; 115:511-15.
4. Morimoto T, Fukui T, Matsushita K, Okawa Y, Shimojyo H, Kusaka S, Tano Y, Fujikado T.

Evaluation of residual retinal function by pupillary constrictions and phosphenes using transcorneal electrical stimulation in patients with retinal degeneration.Graefes Arch ClinExpOphthalmol, 2006, 244 (10): 1283-1292.

5. Fujikado T, Kamei M, Sakaguchi H, Kanda H, Morimoto T, Ikuno Y, Nishida K,Kishima H, Maruo T, KonomaK, Ozawa M, Nishida K. Testing of semichronicallyimplanted retinal prosthesis by suprachoroidal-transretinal stimulation inpatients with retinitis pigmentosa. Invest Ophthalmol Vis Sci. 2011;52:4726-33.
6. Fujikado T, Morimoto T, Kanda H, et al. Evaluation of phosphenes elicited by extraocular stimulation in normals and by suprachoroidal-transretinal stimulation in patients with retinitis pigmentosa. Graefes Arch ClinExpOphthalmol. 2007;245:1411–1419.
7. Morimoto T, Kamei M, Nishida K, SakaguchiH, Kanda H, Ikuno Y, KishimaH,Maruo T, Konoma K, Ozawa M, Nishida K, Fujikado T. Chronic implantation of newly developed suprachoroidal-transretinal stimulation prosthesis in dogs. InvestOphthalmol Vis Sci. 2011 ;52:6785-92.
8. Kanda H, Morimoto T, Fujikado T, et al. Electrophysiological studies of the feasibility of suprachoroidal-transretinal stimulation for artificial vision in normal and RCS rats. Invest Ophthalmol Vis Sci. 2004;45:560–566.
9. Nakauchi K, Fujikado T, Kanda H, et al. Transretinal electrical stimulation by an intrascleral multichannel electrode array in rabbit eyes. Graefes Arch ClinExpOphthalmol. 2005;243:169–174.
10. Nakauchi K, Fujikado T, Kanda H, et al. Threshold suprachoroidal-transretinal stimulation current resulting in retinal damage in rabbits. J Neural Eng. 2007;4:S50–S57.
11. Nishida K, Kamei M, Kondo M, et al. Efficacy of suprachoroidal-transretinal stimulation in a rabbit model of retinal degeneration. Invest Ophthalmol Vis Sci. 2010;51:2263–2268.

,

研究成果の刊行に関する一覧表

1. Miyagawa S, Mihashi T, Kanda H, Hirohara Y, Endo T, Morimoto T, Miyoshi T, and Fujikado T. Asymmetric Wavefront Aberrations and Pupillary Shapes Induced by Electrical Stimulation of Ciliary Nerve in Cats Measured with Compact Wavefront Aberrometer. PLoS One. 2014 Aug 21;9(8):e105615.

2. 神田寛行、不二門尚：電気信号を用いた神経機能再検　人工網膜 (Suprachoroidal-transretinal stimulation STS) 脳21, 18巻1号　pp.84-88、2015

3. 神田寛行、不二門尚：身体補助具の今－クオリティーオブライフの維持に向けて－1．人工網膜　よみがえる光感覚、電気通信学会誌98巻4号　pp.266-271、2015年4月

4. Morimoto T, Kanda H, Miyoshi T, Hirohara Y, Mihashi T, Kitaguchi Y, Nishida K, Fujikado T.: Characteristics of Retinal Reflectance Changes Induced by Transcorneal Electrical Stimulation in Cat Eyes. PLoS One 9(3) Mar. 2014

5. Kanda H, Mihashi T, Miyoshi T, Hirohara Y, Morimoto T, Terasawa Y, Fujikado T: Evaluation of electrochemically treated bulk electrodes for a retinal prosthesis by examination of retinal intrinsic signals in cats. Jpn J Ophthalmol 58(4), pp.309-319, Jul 2014

6. Fujikawa M1, Kawamura H, Kakinoki M, Sawada O, Sawada T, Saishin Y, Ohji M.; Scleral imbrication combined with vitrectomy and gas tamponade for refractory macular hole retinal detachment associated with high myopia. Retina 34(12) pp.2451-7 , 2014 Dec

7. Ichiyama Y1, Sawada T, Kakinoki M, Sawada O, Nakashima T, Saishin Y, Kawamura H, Ohji M.; Anterior chamber paracentesis might prevent sustained intraocular pressure elevation after intravitreal injections of ranibizumab for age-related macular degeneration.　Ophthalmic Res.;52(4) pp.234-238　2014

8. Ueda-Consolvo T, Fuchizawa C, Otsuka M, Nakagawa T, Hayashi A. Analysis of retinal vessels in eyes with retinitis pigmentosa by retinal oximeter. Acta Ophthalmol. 2014 Nov 17 : doi:10.1111/aos.12597.

9. Inoue M, Bissen-Miyajima H, Arai H, Hirakata A: Retinal images viewed through a small aperture corneal inlay. Acta Ophthalmol 92:e168-9, 2014.

10. Khoo HM, Kishima H, Hosomi K, Maruo T, Tani N, Oshino S, Shimokawa T, Yokoe M, Mochizuki H, Saitoh Y, Yoshimine T. Low-Frequency Subthalamic Nucleus Stimulation in Parkinson's Disease: A Randomized, Clinical Trial. Mov Disord. 29 (2) : 270-4, 2014.

11. Hirata M, Morris S, Sugata H, Matsushita K, Yanagisawa T, Kishima H, Yoshimine T. Patient-specific contour-fitting sheet electrodes for electrocorticographic brain machine interfaces. Conf Proc IEEE Eng Med Biol Soc. 5204-7. 2014

12. Suda Y & Kitazawa S. A model of face selection in viewing video stories. Scientific Reports 5: 7666, 2015.

13. Toshihiko Noda, Kiyotaka Sasagawa, Takashi Tokuda, Hiroyuki Kanda, Yasuo Terasawa, Hiroyuki Tashiro, Takashi Fujikado and Jun Ohta, "Fabrication of Fork-Shaped Retinal Stimulator Integrated with CMOS Microchips for Extension of Viewing Angle," Sensors and Materials, Vol. 26, No. 8, pp. 637-648, 2014.

OPEN ACCESS Freely available online

PLOS ONE

Asymmetric Wavefront Aberrations and Pupillary Shapes Induced by Electrical Stimulation of Ciliary Nerve in Cats Measured with Compact Wavefront Aberrometer

Suguru Miyagawa[1,2], Toshifumi Mihashi[3], Hiroyuki Kanda[1], Yoko Hirohara[1,2], Takao Endo[4], Takeshi Morimoto[4], Tomomitsu Miyoshi[5], Takashi Fujikado[1]*

1 Department of Applied Visual Science, Osaka University Graduate School of Medicine, Suita, Osaka, Japan, **2** Topcon Corporation Research Institute, Itabashi, Tokyo, Japan, **3** Innovative Research Initiatives, Tokyo Institute of Technology, Yokohama, Kanagawa, Japan, **4** Department of Opthalmology, Osaka University Graduate School of Medicine, Suita, Osaka, Japan, **5** Department of Integrative Physiology, Osaka University Graduate School of Medicine, Suita, Osaka, Japan

Abstract

To investigate the changes in the wavefront aberrations and pupillary shape in response to electrical stimulation of the branches of the ciliary nerves in cats. Seven eyes of seven cats were studied under general anesthesia. Trains of monophasic pulses (current, 0.1 to 1.0 mA; duration, 0.5 ms/phase; frequency, 5 to 40 Hz) were applied to the lateral or medial branch of the short ciliary nerve near the posterior pole of the eye. A pair of electrodes was hooked onto one or both branch of the short ciliary nerve. The electrodes were placed about 5 mm from the scleral surface. The wavefront aberrations were recorded continuously for 2 seconds before, 8 seconds during, and for 20 seconds after the electrical stimulation. The pupillary images were simultaneously recorded during the stimulation period. Both the wavefront aberrations and the pupillary images were obtained 10 times/sec with a custom-built wavefront aberrometer. The maximum accommodative amplitude was 1.19 diopters (D) produced by electrical stimulation of the short ciliary nerves. The latency of the accommodative changes was very short, and the accommodative level gradually increased up to 4 seconds and reached a plateau. When only one branch of the ciliary nerve was stimulated, the pupil dilated asymmetrically, and the oblique astigmatism and one of the asymmetrical wavefront terms was also altered. Our results showed that the wavefront aberrations and pupillary dilations can be measured simultaneously and serially with a compact wavefront aberrometer. The asymmetric pupil dilation and asymmetric changes of the wavefront aberrations suggest that each branch of the ciliary nerve innervates specific segments of the ciliary muscle and dilator muscle of the pupil.

Citation: Miyagawa S, Mihashi T, Kanda H, Hirohara Y, Endo T, et al. (2014) Asymmetric Wavefront Aberrations and Pupillary Shapes Induced by Electrical Stimulation of Ciliary Nerve in Cats Measured with Compact Wavefront Aberrometer. PLoS ONE 9(8): e105615. doi:10.1371/journal.pone.0105615

Editor: Friedemann Paul, Charité University Medicine Berlin, Germany

Received February 5, 2014; **Accepted** July 25, 2014; **Published** August 21, 2014

Funding: This study was supported by Grant-in-Aid for Scientific Research (25670730) from the Ministry of Education, Culture, Sports, Science and Technology, Japan and by Health Sciences Research Grants (H24-medical device–004) from the Ministry of Health, Labor and Welfare, Japan. The funders had no role in study design, data collection and analysis, decision to publish, or preparation of the manuscript.

Competing Interests: The authors Suguru Miyagawa and Yoko Hirohara are employees of TOPCON company, however, this does not alter the authors' adherence to PLOS ONE policies on sharing data and materials.

* Email: fujikado@ophthal.med.osaka-u.ac.jp

Introduction

Lens accommodation and pupillary dilation or constriction elicited by electrical stimulation of the peripheral nerves or the brain have been extensively studied. The changes in the refractive power of the eye, i.e., accommodation, to electrical stimulation of the ciliary ganglion have been studied in cats and other animals [1–3]. The amplitude of accommodation was dependent on the frequency and voltage of the electrical stimulus. The maximum amplitude of accommodation was about 2 diopters. The accommodative responses elicited by microstimulation of the midbrain or cerebellum have also been studied in cats [4–6]. Glasser et al. demonstrated the accommodative responses elicited by stimulation of the preganglionic Edinger-Westphal nucleus in rhesus monkeys [7,8]. In monkeys, the maximum amplitude of accommodation was 10 to 20 diopters.

The changes in the accommodation not only affected the refractive power but also the ocular aberrations. An ideal monochromatic ray of light from a point source has a perfect spherical wave-front surface. If the eye has an ocular aberration, the wavefront of light reflected from the ocular fundus deviate from an ideal spherical surface, and the deviation in the wavefront is called the wavefront aberrations [9]. Many studies have demonstrated changes in the wavefront aberrations induced by lens accommodation using different techniques in humans. Atchison et al. studied the aberrations with the Howland aberroscope technique [10], and He et al. applied psychophysical ray tracing methods [11]. Recently, Shack-Hartmann wavefront aberrometer (SHWA) techniques allowed the rapid and accurate measurements of the wavefront aberrations [12–14]. With a SHWA, changes of the Zernike terms, e.g., astigmatism, coma, and spherical aberration, can be evaluated during and after accommodative changes. Some studies have demonstrated a significant increase of negative spherical aberration during accommodation using SHWA [15,16]. Animal models have also been used to evaluate changes in the wavefront aberrations with SHWA. For example, Huxlin et al. measured up to sixth order

wavefront aberrations in wake cats [17]. Ramamirtham et al. also measured the wavefront aberrations in young monkeys [18].

The dynamic pupillary dilation and constriction evoked by light stimulation or by electrical stimulation of the ciliary nerve have also been studied in cats [19,20]. In addition, the dynamic pupillary dilations and eye movements in response to microstimulation of the superior colliculus or the optic tectum have been studied in monkeys and birds [21,22]. Dearworth et al. studied the pupillary constriction evoked in vitro by stimulating the ciliary nerve in turtles [23].

Clinically, patients with Adie's syndrome have tonically dilated pupils and accommodative palsy. In addition, the pupillary reactions in these patients are usually segmental due to sector iridoplegia. Bell and Thompson reported that astigmatism was induced with accommodation in one-third of Adie's patients, and they suggested that this may be related to the segmental paralysis of the ciliary muscle [24].

Because both lens accommodation and pupillary constriction and dilation are controlled by postganglionic nerve fibers travelling in the short ciliary nerves, measurements of pupillary diameter and circularity, as well as lens accommodation and wavefront abberrations should be effected by electrical stimulation of the short ciliary nerves. In cats, the short ciliary nerve is made up of a lateral and a medial branch, so segmental stimulation is possible.

The purpose of this study was to determine the dynamic changes in the accommodation, wavefront aberrations, and pupillary size and shape evoked by electrical stimulation of one or both branches of the short ciliary nerve near the posterior pole of the eye in cats. The responses were measured with a custom-made, compact SHWA (Topcon Corporation and Aston University) which allowed us to determine the dynamic changes of accommodation, wavefront aberrations, pupillary size and shape simultaneously [25].

Materials and Methods

Experimental Animals

Seven healthy adult cats between 10- to 14 months-of-age were studied. These cats were raised in a breeding colony in the Institute of laboratory Animals, Osaka University, Graduate School of Medicine. The cats were initially injected with atropine sulfate (0.1 mg/kg) intraperitoneally and after 30 minutes they were anesthetized with an intramuscular injection of ketamine hydrochloride (25 mg/kg). The anesthesia was maintained by a continuous intravenous infusion of pentobarbital sodium (1 mg/kg/hr). The cats were paralyzed by an infusion of pancuronium bromide (0.2 mg/kg/hr) mixed with Ringer's solution and glucose (0.1 g/kg/hr), and artificially ventilated with equivalent mixture of nitrous oxide (N^2O) and oxygen (O^2) for auxiliary anesthesia and alleviation of pain.

The end-tidal CO^2 concentration was controlled at 3.5 to 5.0% by altering the frequency and tidal volume of ventilation. The intratracheal pressure and electrocardiogram were also monitored, and the body temperature was maintained at 38°C with a heating pad. The cornea of cats was kept moist using custom made contact lenses during the experiments.

This study was carried out in strict accordance with the recommendations in the Guide for the Care and Use of Animals of the National Institutes of Health. The procedures were approved by the Animal Research Committee of the Osaka University Medical School, document number 20–145. All surgery was performed under pentobarbital sodium anesthesia, and all efforts were made to minimize pain. All animals were sacrificed by a rapid intravenous infusion of pentobarbital sodium (64.8 mg/ml) after a completion of all experimental procedures.

Electric Stimulation of Ciliary Nerve

In cats, the ciliary ganglion gives rise to a lateral and a medial branch of the short ciliary nerve. Additionally, one or two fine communicating branches from the long ciliary nerve are fused with the short ciliary nerve. Electrical currents were applied to either the lateral or medial branch or to both branches of the short ciliary nerves to study the changes in the accommodation, pupillary size and shape, and wavefront aberrations. A schematic diagram of the experimental setup is shown in Figure 1. The stimulating electrodes were bipolar hook-shaped electrodes made of 0.3 mm diameter stainless steel wire (OK212-069, Unique Medical, Tokyo, Japan). The wire was coated with insulating resin with a small region of the tip bared where the electrode contacted the ciliary nerve. The electrodes were hooked onto the branch of the short ciliary nerve about 5 mm from sclera. Trains of monophasic square wave electrical pulses were applied to either the lateral or the medial or to both branches of the short ciliary nerve. All pulses were generated by an isolated pulse generator (STG2008, Multi Channel Systems MCS GmbH, Reutlingen Germany). The pulse parameters were: current intensities of 0.1, 0.3, 0.5, and 1.0 mA; frequencies of 5, 10, 20, and 40 Hz; pulse duration of 0.5 ms/phase; and the duration of the pulse trains was 8 s. Changes in the accommodation, wavefront aberrations and pupillary shape evoked by electrical stimulation of short ciliary nerve were simultaneously recorded with a compact wavefront aberrometer.

Dynamic Measurements of Wavefront Aberrations Using Compact Wavefront Aberrometer

The wavefront aberrations were measured with a compact wavefront aberrometer. This device consisted of an open-field dichroic mirror and a cuboid shaped body (12×12×4.5 cm), which can be attached to a standard flex holder (Figure 1). Because of the flexibility and compactness of this aberrometer, it

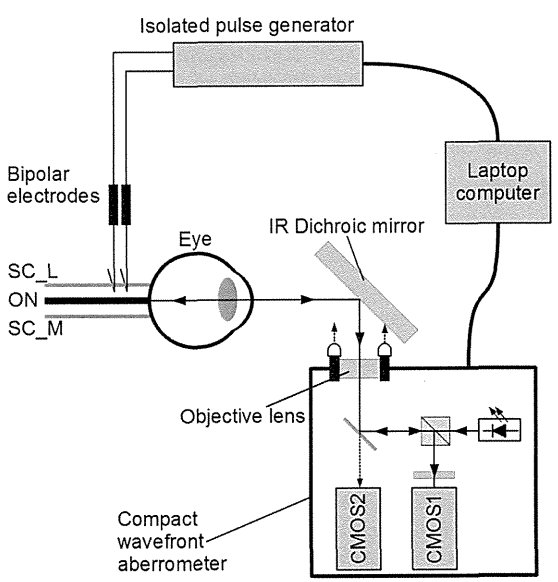

Figure 1. Photograph of the compact wavefront aberrometer attached to a flex holder arm.
doi:10.1371/journal.pone.0105615.g001

can be easily used for *in vivo* animal studies or clinical studies. The experimental setup and optical arrangement are shown in Figure 2. The aberrometer contained two complementary metal-oxide semiconductor (CMOS) image sensors. The wavefront aberrations were measured with the first CMOS sensor (CMOS1). A lenslet array plate located in front of CMOS1 focused the Shack-Hartmann spot images. The digitized Shack-Hartmann spot images were recorded sequentially at 10 frames/sec. Therefore, we were able to measure the changes of accommodation and aberrations every 100 ms. The digitized Shack-Hartmann spot images were analyzed quantitatively for up to the 6th order by expanding the set of Zernike polynomials with custom written software.

The second CMOS sensor (CMOS2) obtained the images of the anterior segment of the eye to evaluate the pupillary shape. Both the aberrometer and the isolated pulse generator were synchronously controlled by a commercially available laptop computer.

The accommodative responses were assessed by the changes of the refractive power (spherical equivalents). The wavefront aberrations were evaluated by the changes of the Zernike coefficients, and the wavefront aberrations were specified using the standard nomenclature defined with reference to the standard coordinate system recommended by the Optical Society of America [26]. A color map diagram of Zernike polynomials of up to 4th order is shown in Figure 3. The with- and against-the-rule astigmatism (Z^{2}_{2}), the oblique astigmatism (Z^{-2}_{2}), the trefoil terms (Z^{-3}_{3} and Z^{3}_{3}), the x coma (Z^{1}_{3}), the y coma (Z^{-1}_{3}), and spherical aberration term (Z^{0}_{4}) were determined.

To study the dynamic changes of accommodation, we determined the velocity of the accommodative responses where the velocity was defined in diopters/sec and we assessed the maximum amplitude of accommodation and the time required to reach 80% of the maximum amplitude. Then the velocity ratio was calculated as 80% of maximum amplitude divided by the time to reach this level, i.e., 0.8 amplitude of accommodation in diopters/time in msec. In cases where the wavefront aberration

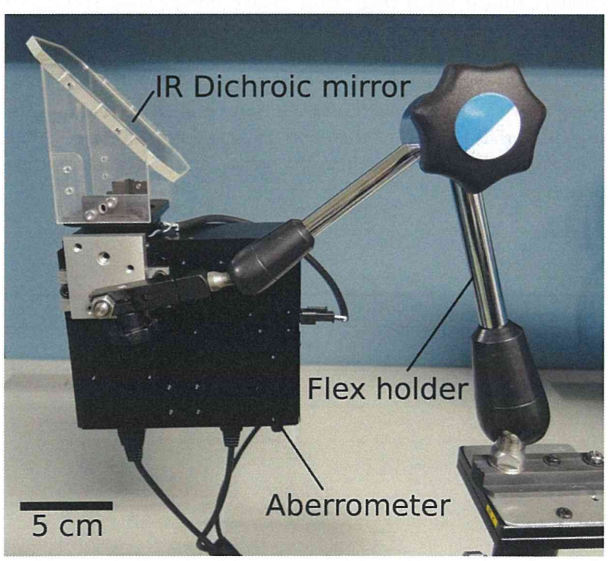

Figure 2. Schematic diagram of experimental setup. ON, optic nerve; SC_L, lateral branch of the short ciliary nerve; SC_M, medial branch of the short ciliary nerve. CMOS1, complementary metal-oxide semiconductor (CMOS) image sensor for Shack-Hartmann spot image; CMOS2, CMOS image sensor for anterior eye (pupil) image.
doi:10.1371/journal.pone.0105615.g002

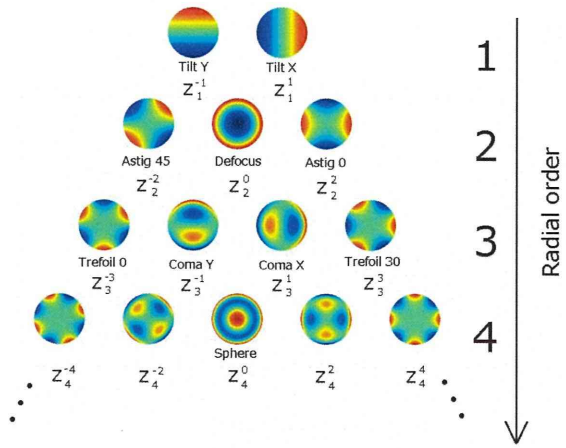

Figure 3. Color map diagram of Zernike polynomials up to the 4th order. Astig 45, oblique astigmatism (45 deg); Astig 0, with-the-rule astigmatism (0 deg); Trefoil 0, vertical trefoil aberration (0 deg); Trefoil 30, oblique trefoil aberration (30 deg); Sphere, spherical aberration.
doi:10.1371/journal.pone.0105615.g003

was not measureable due to pupillary constriction, the pupil was dilated by 5% phenylephrine HCl (Neosynesin). Earlier studies showed that 10% neosynephrine eye drops did not alter the accommodation in cats [27].

Measurements of Pupillary Shape

To study pupillary dilation and constriction, the pupil was photographed by CMOS image sensor incorporated into the wavefront aberrometer. The images were analyzed with a custom written software. The contour of the pupil was first outlined to calculate the area of the pupil (mm^2) and to evaluate the pupil shape. The coordinates of the center of gravity of the pupil were also calculated to determine whether there was an asymmetrical change in the pupillary shape. This program can determine both the size and shape of the pupil. To study the relationship between the changes in the wavefront aberrations and pupillary shape, both were recorded simultaneously and sequentially at 10 frames/sec for 2 seconds before, 8 seconds during, and for 20 seconds after the stimulation. The ambient illumination of light was kept steadily during measurements to avoid changing pupil size due to pupillary reaction to light.

Statistical Analyses

Data were statistically analyzed using commercial software (SigmaPlot, version 12.0; HULINKS, Inc.). Comparisons between two groups were made by Student's *t* tests. The level of statistical significance was set at $P<0.05$. To analyze the degree of association between velocity and maximum amplitude of accommodation, Pearson's correlation coefficient was calculated.

Results

Amplitude of Accommodation

The average amplitude of accommodation due to stimulation of the medial or the lateral ciliary nerves was 0.64±0.34 D (mean ± standard deviations) by a stimulation of the medial or lateral branch of ciliary nerve with a range of 0.25 to 1.19 D (Table 1). The amplitude of accommodation increased with increasing currents and frequencies of stimulation (Figure 4). However,

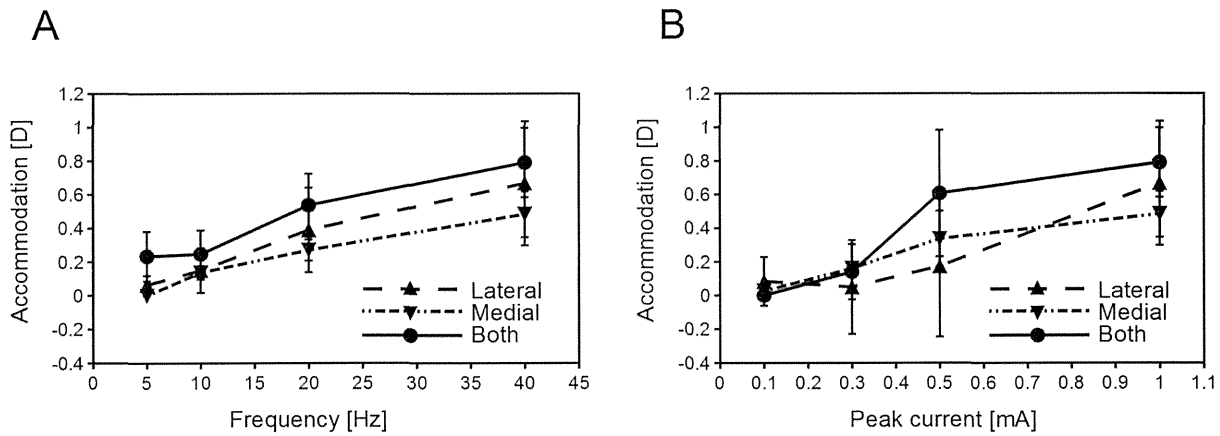

Figure 4. Maximum amplitude of accommodation as a function of the frequency (A) or current (B) of the stimulus. A: The frequency was varied and the current was fixed at 1 mA. B: The current was varied and the frequency was fixed at 40 Hz. One or 2 drops of phenylephrine hydrochloride was instilled prior to the measurements. The maximum amplitude of accommodation is the average of four eyes of four cats (Cat #2, #4, #6, #7). Error bars indicates standard deviations. Monophasic square pulses at a fixed pulse width of 0.5 ms were applied to the lateral, medial, or both branches of the short ciliary nerve.
doi:10.1371/journal.pone.0105615.g004

increasing the currents >1 mA or the frequencies >40 Hz did not increase the amplitude of accommodation significantly. When both branches of the ciliary nerve were stimulated, the accommodative responses were greater than when only one branch was stimulated in 3 of 4 cats.

Dynamic Accommodative Responses

The accommodative responses were obtained by a sequential recording of the wavefront aberrations. The latency of accommodation was always shorter than the detection limit, <100 ms, of our instrument. The accommodation amplitude continued to change during the 4 seconds after the onset of stimulation (Figure 5A). With longer stimulus durations, the amplitude of accommodation reached and maintained a steady state during the stimulation (Figure 5B). After the stimulation, the accommodation decreased slowly to the original level within 10 sec.

The velocity of accommodation varied among the trials. A comparison of the velocities of accommodation and the maximum amplitude of accommodation are shown in Figure 6. The velocities increased significantly with increasing maximum accommodation (Pearson's correlation; $r = 0.839$, $P<0.001$).

Dynamic Pupillary Dilation

The pupil dilated asymmetrically when one branch of the ciliary nerve was stimulated, but if both branches of the ciliary nerve were stimulated, the pupil dilated symmetrically. The pupil never constricted in response to the stimulation parameters used. Representative images of the pupils are shown in Figure 7. The pupillary image before stimulation is shown in Figure 7A. Stimulating the lateral branch (7B) or the medial branch (7C) of the short ciliary nerve produced asymmetric dilation. The pupillary image when both short ciliary nerves were stimulated by the same parameters is shown in Figure 7D.

The time course of the pupillary dilation is shown in Figure 8. The pupil dilated laterally in the case of lateral branch of the short ciliary nerve was stimulated and the pupil dilated medially in the case of medial branch of the short ciliary nerve was stimulated. The pupil dilated symmetrically when both branches were stimulated (n = 2).

Table 1. *Maximum accommodative response.*

	Maximum Accommodative Response (Diopter)		
No.	**Lateral**	**Medial**	**Both**
#1	1.08	0.88	
#2	0.25	0.46	0.67
#3	1.19	0.30*	
#4	0.80*	0.36*	1.01*
#5	0.58*	0.20*	
#6	0.95*	0.63*	0.60*
#7	0.18*	0.20*	0.41*

Trains of monophasic square pulses were applied to the lateral, medial or both branches of the short ciliary nerve(1 mA, 40 Hz, 8 sec). The maximum accommodative amplitudes were evaluated by the changes in the refractive power.
*: 1 or 2 drops of Phenylephrine Hydrochloride was instilled.
doi:10.1371/journal.pone.0105615.t001

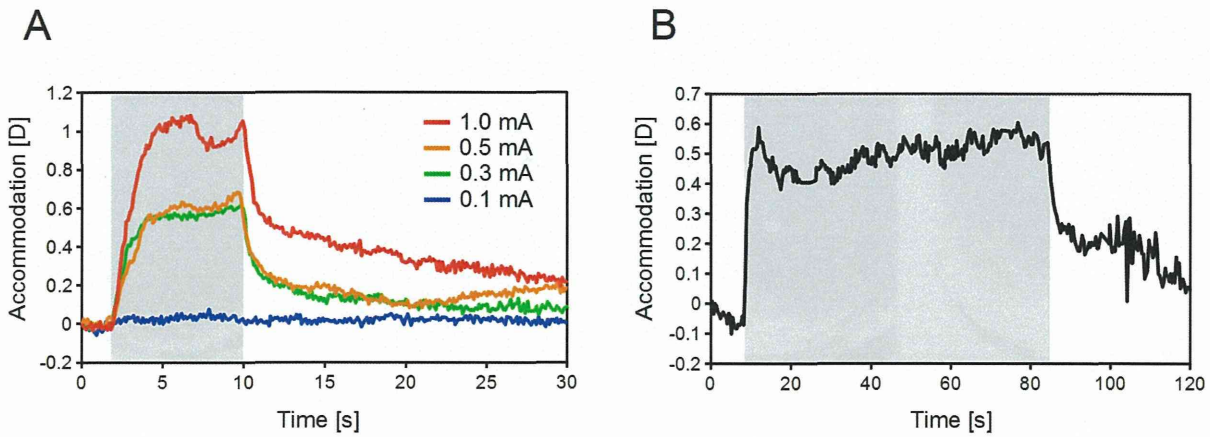

Figure 5. Effect of current and stimulus duration on accommodative responses. A: Typical accommodative responses (Cat #1). Trains of monophasic square pulses of different currents were applied to the lateral branch of the short ciliary nerve. The pulse width and frequency were fixed at 0.5 ms and 40 Hz respectively. B: Efffect of continuous stimulation. A current of 1 mA, frequency of 20 Hz, and duration of pulse train of 75 sec were applied. Shaded areas: Time stimulation was applied.
doi:10.1371/journal.pone.0105615.g005

The latencies of the pupillary responses were always shorter than the detection limit (less than 100 ms). After the stimulation, the pupil gradually returned to the original state within several tens of seconds.

Wavefront Aberrations

The wavefront aberrations changed with accommodation. A typical example of the time course of the Zernike coefficients and accommodative responses are shown in Figure 9. The time courses of changes in Zernike terms were similar to those of the accommodative responses. The averages and standard deviations of the Zernike coefficients in the seven cats are shown in Figure 10. Zernike coefficients up to 6th order can be calculated with our software. However, the 4 to 6th order of the Zernike terms except for spherical aberration term (Z^0_4) are not shown in the results because these terms changed only slightly in almost all trials. The changes of the Zernike coefficients were determined by subtracting the maximum value during the stimulation from the pre-stimulation value. The stimulation parameters were fixed with a peak current of 1 mA, frequency of 40 Hz, and pulse width of 0.5 msec.

We compared the findings between stimulating the lateral and medial branches of the short ciliary nerve. Significant statistical differences were found in the oblique astigmatism term. However, significant statistical differences were not found for all of the other Zernike terms.

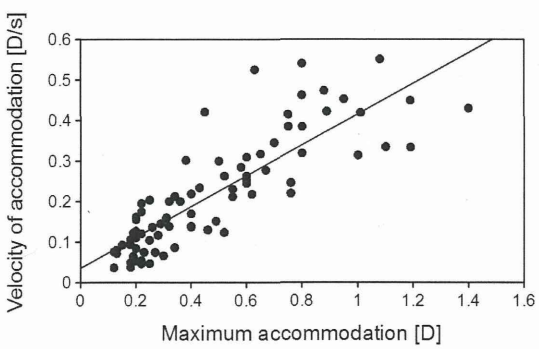

Figure 6. Changes in the velocity of accommodation as a function of maximum accommodation. Stimulus was applied to the lateral or medial or both branches of the ciliary nerve. The data from all seven cats are plotted. Correlations between the velocity of accommodation and maximum accommodation made by Pearson's correlation ($r = 0.839$, $P < 0.001$).
doi:10.1371/journal.pone.0105615.g006

Discussion

Our results showed that stimulation of the short ciliary nerve leads to simultaneous changes in the accommodation, pupillary diameter, and wavefront aberrations. The pupil was never constricted during the stimulation of the branches of short ciliary nerve. Lens accommodation is under the control of the parasympathetic system, while the pupil is under the control of the sympathetic system. Our findings indicate that the nerve bundles which were stimulated contained both sympathetic and parasympathetic nerve fibers. In fact, Kuchiiwa et al. showed in their anatomical studies that the short and long ciliary nerves fuse close to the eye in both the medial and lateral divisions of the short ciliary nerve [28,29]. The other possible cause of these responses is due to stimulating the sensory nerve in the short ciliary nerve.

The amplitude of accommodation increased with an increase in the frequency and the current of stimulation (Figure 4). The maximum amplitude of accommodation was 1.19 diopters, and increasing the currents >1.0 mA and frequencies >40 Hz did not increase the amplitude of accommodation.

In earlier studies, the maximum accommodation in cats was around 2 diopters when the ciliary ganglion was stimulated [1–3]. In addition, the near point of physiological accommodation in cats was estimated to be between 25 to 36 cm or 2.8 to 4.0 D [30]. The maximum amplitude of accommodation under our conditions was less than these values. This disagreement might be caused by the contact between hook shaped electrodes and nerve bundle, and the hook electrodes placed on the nerve bundle might have stimulated only a part of it.

The latencies of accommodation were always less than the detection limit of our recording system (Figure 5). Earlier studies showed that the latencies were >200 ms in the case of ciliary ganglion or midbrain stimulation in cats [27,31,32]. This

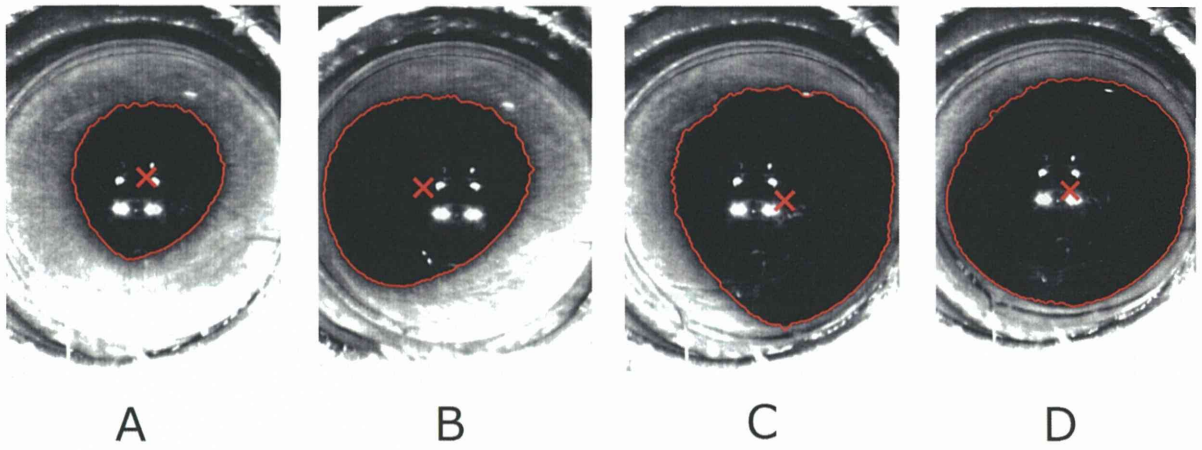

Figure 7. Pupillary images before and after electrical stimulation of the ciliary nerve (Cat #2 right eye). A: Before stimulation. B: Maximum dilation when the lateral branch of the short ciliary nerve was stimulated. C: Maximum dilation when medial branch was stimulated. D: Maximum dilation when both side of branch was simultaneously stimulated. Solid line: Detected contour of the pupil. X: The center of the pupil that is represented as the center of gravity that was calculated from contour data.
doi:10.1371/journal.pone.0105615.g007

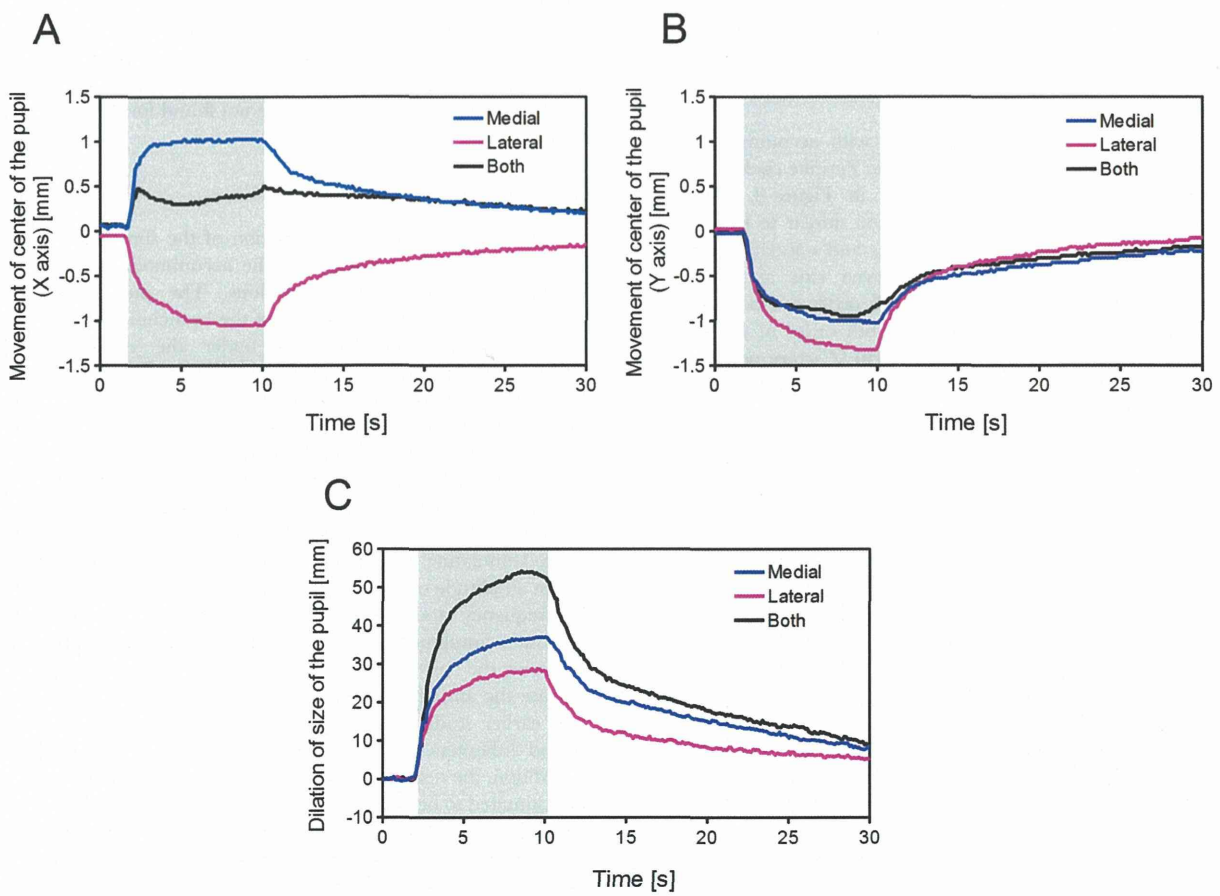

Figure 8. Time course of the changes in the pupillary response to electrical stimulation of one or both branches of the short ciliary nerve (Cat #2). A: Horizontal movement of the center of the pupil. The direction of medial side is represented by positive x-axis, the lateral side is represented by negative x-axis. B: Vertical movement of the center of the pupil. The superior direction is represented by upward dilation, and the inferior direction is represented by downward dilation. C: Changing of the pupil size calculated from the detected contour data. Shaded areas: Stimulation (the pulse train was continuously applied).
doi:10.1371/journal.pone.0105615.g008

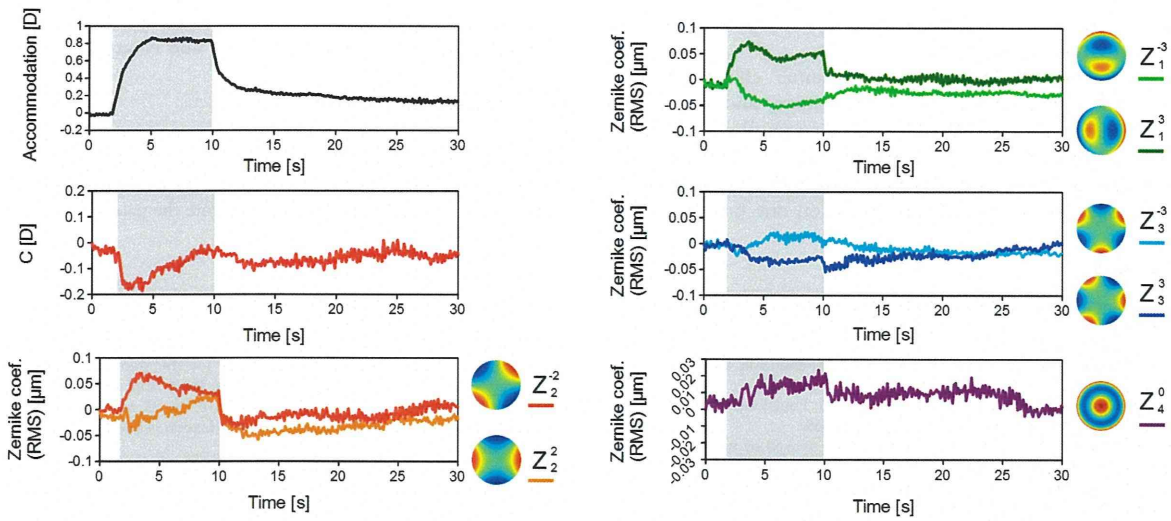

Figure 9. The time course of the changes in the Zernike coefficients and accommodative changes. (Cat #1) S. E.: Spherical Equivalent of refractive change, C: Cylindrical value. All data are the values of the change from the initial state. Shaded areas: Stimulation (the pulse train is continuously applied). The current of 1 mA, the frequency of 40 Hz, the duration of pulse train of 8 seconds were applied to the lateral branch of the short ciliary nerve.
doi:10.1371/journal.pone.0105615.g009

discrepancy might be caused by a difference of the stimulation sites.

The maximum velocity of accommodation was 0.6 D/s in this study taking 4 seconds to reach the peak of accommodation (Figure 4). In addition, we found that the velocity of accommodation was significantly correlated with the amplitude of accommodation (Figure 6). This is in good agreement with previous studies in humans and rhesus monkeys [7,8,33]. The latencies might depend on the region stimulated, and the velocity of accommodation may depend on the mechanical properties of the ciliary body and the crystalline lens.

The pupil was asymmetrically dilated when one branch of the ciliary nerve was stimulated (Figures 7 and 8). This suggests that each branch innervates localized areas of the dilator muscle of the pupil. Asymmetric pupillary dilation indicates that the ciliary muscle may also be asymmetrically constricted by stimulation of the short ciliary nerve on one side. If ciliary muscle constricted asymmetrically, asymmetric terms of wavefront aberrations should be changed.

In all trials, the pupil was dilated or was kept stable in size, but never constricted to any of the stimulation parameters. This might be explained by a concurrent stimulation of both parasympathetic and sympathetic nerve fibers. In cats, the sympathetic fibers are reported to be incorporated in the short ciliary nerves after the nerves have been joined by the long ciliary nerves somewhere between the ciliary ganglion and the eye [34]. At the area of the branch of short ciliary nerve which was stimulated in this study, about 5 mm from sclera, the parasympathetic and sympathetic fibers might be mixed. Our results indicated that the stimulation of mixed sympathetic and parasympathetic fibers will cause a dilation. The discharge rate of the mixed ciliary nerve is increased with spontaneous pupillary dilation in cats [35].

The wavefront aberrations change with accommodation in humans, and the spherical aberration (Z^0_4) shows the greatest change among all the Zernike terms [12]. The changes in the astigmatism and the coma terms were smaller than that for spherical aberration. In contrast, the changes in the spherical aberration was smaller than for the astigmatism and coma terms (Figures 9 and 10). These discrepancies may be due to differences in the shape of the crystalline lens between humans and cats. The crystalline lens of cats is more spherical in shape than that of humans.

The differences in the changes in the oblique astigmatism term (Z^{-2}_2) between stimulation of the lateral or the medial branch of the short ciliary nerve were significant (Figure 10). This suggests that an asymmetrical constriction of ciliary muscle is induced by unilateral ciliary nerve stimulation, which may induce the deformation of crystalline lens. In patients with Adie's syndrome, astigmatism is reportedly induced after accommodation [23]. Our findings in cats support the hypothesis that a segmental constriction of ciliary muscle occurs when patients with Adie's syndrome accommodates which eventually causes the increase of asymmetrical astigmatism.

Further study is necessary to confirm the localized innervation of the short ciliary nerve that lead to the asymmetric contraction of the ciliary muscle. It is also necessary to make a computer

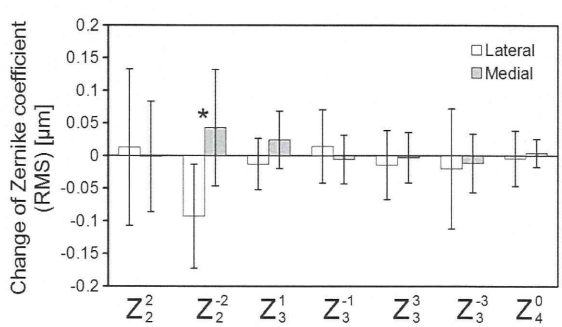

Figure 10. The average change of Zernike coefficients among the seven cats. Error bars represent the standard deviations. A current of 1 mA, frequency of 40 Hz, and duration of pulse train of 8 seconds were applied. Comparisons between the two cases (lateral or medial branch of short ciliary nerve stimulation) were made by Student's *t* tests. The level of statistical significance was set as $P<0.05$. (*: $P<0.05$).
doi:10.1371/journal.pone.0105615.g010

simulation if the asymmetric movement of ciliary muscle induces the deformation of crystalline lens.

In conclusion, we measured the dynamic change of the wavefront aberrations, pupillary size and shape, and accommodation simultaneously and serially with a custom-built compact wavefront aberrometer. The asymmetric pupillary dilation and asymmetrical changes of the wavefront aberrations with accommodation elicited by electrical stimulation on one branch of the ciliary nerve suggest that the branch of ciliary nerve innervates localized regions of the dilator of pupil and ciliary muscle.

Author Contributions

Conceived and designed the experiments: SM HK YH TE TF T. Miyoshi T. Morimoto T. Mihashi. Performed the experiments: SM HK YH TE TF T. Miyoshi. Analyzed the data: SM YH. Contributed reagents/materials/analysis tools: SM HK YH T. Miyoshi. Wrote the paper: SM YH TF.

References

1. Marg E, Reeves JL, Wendt WE. (1954) Accommodative response of the eye to electrical stimulation of the ciliary ganglion in cats. Am. J. Opthom. and Arch Am Acad Opthom 31: 127–137.
2. Ripps H, Breinin GM, Baum JL. (1961) Accommodation in the cat. Tr Am Ophth Soc 59: 176–193.
3. Ripps H, Siegel IM, William BG, Getz WB. (1965) Functional organization of ciliary muscle in the cat. Am J Physiol 203: 857–859.
4. Sawa M, Ohtsuka K. (1994) Lens accommodation evoked by microstimulation of the superior colliculus in the cat. Vision Res 34: 975–981.
5. Konno S, Ohtsuka K. (1997) Accommodation and pupillconstriction areas in the cat midbrain. Jpn J Opthalmol 41: 43–48.
6. Hosoba M, Bando M, Tsukahara N. (1978) The cerebellar control of accommodation of the eye in the cat. Brain Res 153: 495–505.
7. Vilupuru AS, Glasser A. (2002) Dynamic accommodation in rhesus monkeys. Vision Res 42: 125–141.
8. Ostrin LA, Glasser A. (2007) Edinger-Westphal and pharmacologocally stimulated accommodative refractive changes and lens and ciliary process movements in rhesus monkeys. Exp Eye Res 84: 302–313.
9. Thibos LN, Bradley A, Still DL, Zhang X, Howarth PA. (1990) Theory and measurement of ocular chromatic aberration. Vision Res 30: 33–49.
10. Atchison DA, Collins MJ, Wildsoet CF, Christensen J, Waterworth MD. (1995) Measurement of monochromatic ocular aberrations of human eyes as a function of accommodation by the howland aberroscope technique. Vision Res 35: 313–323.
11. He JC, Burns SA, Marcos S. (2000) Monochromatic aberrations in the accommodated human eye. Vision Res 40: 41–48.
12. Liang J, Williams DR. (1997) Aberrations and retinal image quality of normal human eye. J Opt Soc Am A 14: 2873–2883.
13. Porter J, Guirao A, Cox IG, Williams DR. (2001) Monochromatic aberrations of the human eye in a large population. J Opt Soc Am A 18: 1793–1803.
14. Thibos LN, Hong X, Bradley A, Cheng X. (2002) Statistical variation of aberration structure and image quality in a normal population of healthy eyes. J Opt Soc Am A 19: 2329–2348.
15. Chang H, Barnett JK, Vilupuru AS, Marsack JD, Kasthurirangan S, et al. (2004) A population study on changes in wave aberrations with accommodation. J Vis 4: 272–280.
16. Ninomiya S, Fujikado T, Kuroda T, Maeda N, Tano Y, et al. (2002) Changes of ocular aberration with accommodation. Am J Opthamol 134: 924–926.
17. Huxlin KR, Yoon G, Nagy L, Porter J, Williams D. (2004) Monochromatic ocular wavefront aberrations in the awake-behaving cat. Vision Res 44: 2159–2169.
18. Ramamirtham R, Kee C, Hung LF, Qiao-Grider Y, Huang J, et al. (2007) Wave aberrations in rhesus monkeys with vision-induced ametropias. Vision Res 47: 2751–2766.
19. Terdiman J, Smith JD, Stark L. (1969) Pupil response to light and electrical stimulation: static and dynamic characteristics. Brain Res 16: 288–292.
20. Watanabe T, Koike N, Inoue T, Kondo Y, Yanagaki H, et al. (1990) An automated simultaneous recording system for the pupillary movement and unitary discharge of the ciliary nerve in cats. Jpn J Appl Phys 29: 445–452.
21. Wang C, Boehnke SE. White BJ, Munoz DP. (2012) Microstimulation of the monkey superior colliculus induces pupil dilation without evoking saccades. J Neurosci 32: 3629–3636.
22. Netser S, Ohayon S, Gutfreund Y. (2010) Multiple manifestations of microstimulation in the optic tectum: Eye movements, pupil dilations, and sensory priming. J Neurophysiol 104: 108–118.
23. Dearworth JR, Brenner JE, Blaum JF, Littlefield TE, Fink DA, et al. (2009) Pupil constriction evoked in vitro by stimulation of the oculomotor nerve in the turtle (Trachemys scripta elegans). Vis Neurosci 26: 309–318.
24. Bell RA, Thompson HS. (1978) Ciliary muscle dysfunction in Adie's syndrome. Arch Ophthalmol 96: 638–42.
25. Bhatt UK, Sheppard AL, Shah S, Dua HS, Mihashi T, et al. (2013) Design and validity of miniaturized open-field aberrometer. J Cataract Refract Surg 39: 36–40.
26. Thibos LN, Applegate RA, Schwiegerling JT, Webb R, VSIA Standard Taskforce Members. (2002) Standards for reporting the optical aberations of eyes. J Refract Surg 18: S652–S660.
27. O' Neill WD, Brodkey JS. (1970) A nonlinear analysis of the mechanics of accommodation. Vision Res 10: 375–391.
28. Kuchiiwa S, Kuchiiwa T, Suzuki T. (1989) Comparative anatomy of accessory ciliary ganglion in mammals. Anat Embryol 180: 199–205.
29. Kuchiiwa S. (1990) Morphology of the accessory ciliary ganglion of the cat. Anat Embryol 181: 299–303.
30. Bloom M, Berkley MA. (1977) Visual acuity and the near point of accommodation in cats. Vision Res 17: 723–730.
31. Bando T, Tsukuda K, Yamamoto N, Maeda J, Tsukahara N. (1981) Mesencephalic neurons controlling lens accommodation in the cat. Brain Res 213: 201–204.
32. Bando T, Takagi M, Toda H, Yoshizawa T. (1992) Functional roles of the lateral supersylvian cortex in ocular near response in the cat. Neurosci Res 15: 162–178.
33. Bharadwaj SR, Schor CM. (2004) Acceleration characteristics of human ocular accommdation. Vision Res 45: 17–28.
34. Christensen K. (1936) Sympathetic and parasympathetic nerves in the orbit of the cat. J Anat 70(Pt 2): 225–232.
35. Ashe JH, Cooper CL. (1977) Multifiber effect activity in postganglionic sympathetic and parasympathetic nerves related to the latency of spontaneous and evoked pupillary dilation. Exp Neurology 59: 413–434.

特集3

電気信号を用いた神経機能再建

人工網膜 (suprachoroidal-transretinal stimulation: STS)

神田寛行（かんだひろゆき），不二門 尚（ふじかどたかし）
大阪大学大学院医学系研究科感覚機能形成学教室（〒565-0871 大阪府吹田市山田丘2-2）

SUMMARY

視覚神経系への電気刺激により，視機能を再建する医療機器「人工網膜」の研究開発が進められている．その仕組みは，眼の代わりに眼鏡枠に取り付けた小型カメラで外界の画像を撮影し，画像データを基に刺激電流を生成し，網膜近傍に設置した多極電極を介して網膜を電気刺激することで人工の視覚を作る．すでに臨床試験が各国で行われており，近い将来の実用化が期待されている．わが国では，2001年より大阪大学を中心に人工網膜の開発プロジェクトがスタートし，独自の刺激方式であるsuprachoroidal-transretinal stimulation（STS）方式を採用した人工網膜の開発が進められている．現在，第二世代型STS人工網膜が完成し，その臨床試験が実施されている．

KEY WORDS
人工網膜
人工視覚
神経インタフェース
視覚再建

はじめに

網膜への電気刺激により生じる擬似的な光感覚を利用して，人工的に視覚を再建する医療機器「人工網膜」の開発が国内外で進められている．人工網膜の対象は網膜色素変性をはじめとする視細胞が退行変性する網膜変性疾患である．本稿では，著者らが開発を進めるsuprachoroidal-transretinal stimulation（STS）方式の人工網膜を中心に，人工網膜のしくみと現在の研究状況について紹介する．

I. 網膜色素変性

人工網膜の主な対象疾患は網膜色素変性である．初期には夜盲を自覚し，視野狭窄および視力低下が徐々に進行し，重度の場合には失明に至ることもある．現在の医療の現場では，治療法は皆無で，わが国における中途失明原因の第三位を占める[1]．

通常，健常な網膜では，網膜に到達した眼内入射光が視細胞で神経信号へと変換され，双極細胞，網膜神経節細胞へと順に伝達される．一方，末期の網膜色素変性の場合，光受容器である視細胞が広範囲に退行性変性するために，眼内入射光を神経信号に変換することができない．しかし病態が進行した場合でも網膜神経節細胞などの網膜内層の神経細胞が残存することが

1344-0128/15/¥100/JCOPY

知られている[2]．したがって，網膜内層の神経細胞をターゲットとして電気刺激を与えることで同細胞の神経活動を人工的に誘発し，これが視覚中枢に伝わることで擬似的な光感覚「electrical phosphene」が生まれる．

II. 人工網膜の仕組み

人工網膜は，人工的な方法で光を受光し，光を電気信号に変換し，電気信号を網膜内の視細胞以外の神経細胞に伝達して人工的に光感覚を生みだす装置と定義されている[3]．具体的には，カメラで得た外界の画像情報に合わせて網膜近傍に埋植した多極電極で複数のelectrical phosphene を生み出してパターンを作製する（**図 1**）．

世界的にみて，人工網膜の研究が本格的に始まったのは 1990 年代以降である．当初は主にアメリカやドイツの研究グループが中心となり研究を進めていたが，2000 年代に入り日本をはじめオーストラリアや韓国も参入するようになった．

現在までに考案されてきた人工網膜は多極電極の埋植位置によって，網膜上刺激方式，網膜下刺激方式，STS 方式に大別される（**図 2**）．

網膜上刺激方式は多極電極を網膜の上側に設置して網膜を刺激する方式である．この方式の中で最も開発が進んでいるのが Second Sight Medical Products 社（米国）の“Argus Ⅱ”である．これは南カリフォルニア大学の Humayun らの研究が基となって開発された人工網膜である．これまでに 30 名以上の網膜色素変性患者に対して多施設臨床試験が実施された[4]．Argus Ⅱは 2011 年に CE マークを取得し EU 圏内での販売が認められた．さらに 2013 年には米国食品医薬品局（FDA）の認可を受けアメリカ国内での販売が認められた．

網膜下刺激方式は，多極電極を網膜と脈絡膜の間に設置して網膜を刺激する方式である．この方式の中で最も開発が進んでいるのが，Retinal Implant 社（ドイツ）の“Alpha IMS”とよばれる人工網膜である．これはチュービンゲン大学の Zrenner らの研究成果によって開発された人工網膜である[5]．このデバイスには多極電極基板上に 1,500 個の素子が組み込まれ，各素子は受光素子と増幅器と刺激電極で構成されている．これにより多極電極で撮像と電気刺激を同時に行うことができる．これまでの臨床試験で約 20 例の手

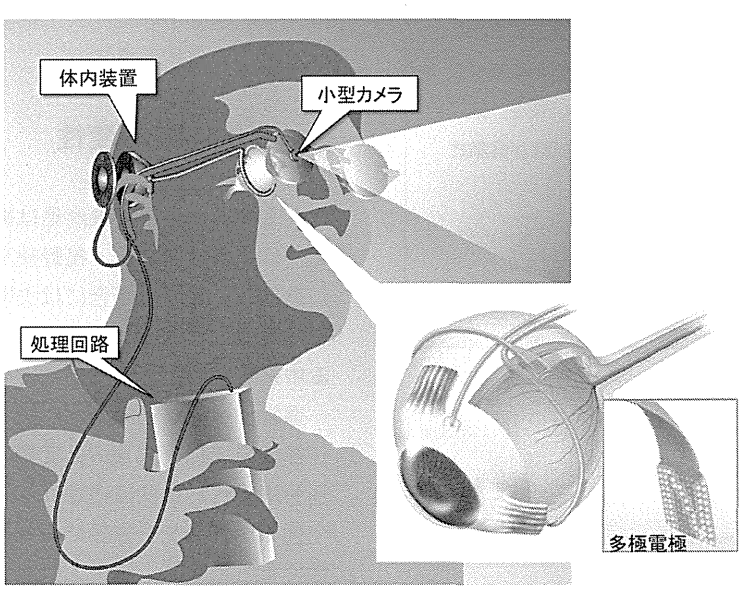

図 1　人工網膜の全体システム
（p.6 カラー図参照）

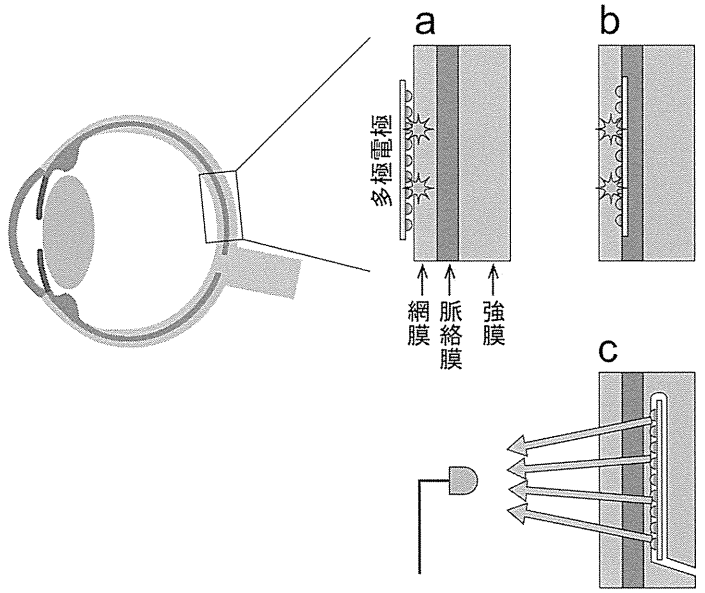

図 2　人工網膜の三つの方式
a：網膜上刺激方式．b：網膜下刺激方式．c：STS 方式．（p.7 カラー図参照）

術が実施された．さらなる臨床試験が，ドイツ，英国，香港などで実施されている．すでに CE マークを取得しており，EU 圏内での販売が認められた．また，米国における販売に向け現在 FDA にて審査が行われている．

STS 方式は多極電極を脈絡膜よりも外側に設置し網膜を刺激する．本方式の詳細は次章にて説明する．

III.　STS 方式の人工網膜の開発状況

わが国では，2001 年度に大阪大学の故田野教授（当時）をグループリーダとして大阪大学，奈良先端科学技術大学院大学，（株）ニデックなど複数の研究機関が参加して人工網膜の開発プロジェクトが立ち上がった．当初は網膜上刺激型あるいは網膜下刺激型の人工網膜の検討が進められていたが，両者ともに多極電極が網膜組織に直接接触するために手術時の網膜損傷のリスクが高い．これらの問題を回避するために，当プロジェクトで新しい刺激方式が考案された．それが STS 方式である．

STS 方式では電極を脈絡膜よりも外側に設置し，帰還電極を硝子体腔中に設置して両電極間で通電する．電極が網膜と直接接触しないため，手術時の網膜損傷のリスクが他の方式よりも低い．ほかにも，網膜への広い範囲に電極を埋植できる点や，再生医療との併用が可能な点が STS 方式の利点としてあげられる．

さまざまな非臨床試験を通じて STS 方式の実現可能性が示された[6,8]ことから，2004 ～ 2008 年にわたり，合計 4 名の網膜色素変性患者に対して急性臨床試験が実施された．試験の結果，網膜色素変性症例に対して STS 方式により限局した electrical phosphene が得られることが確認された[9]．

IV.　第一世代型 STS 方式人工網膜システム

次のステップとして，当プロジェクトは体内への慢性埋植が可能なデバイスの開発に着手した．当時，国内にペースメーカーや人工内耳など電子医療機器の体内インプラントのメーカはなく，開発はゼロからのスタートだった．多くの時間と労力を要したが，2010 年に体内埋植可能なデバイスの試作に成功した．このデバイスには 9 極型の多極電極が搭載された（**図 3**）．